

# NASA-ISRO Synthetic Aperture Radar (NISAR) Mission

Kent Kellogg\*  
 Pamela Hoffman\*  
 Shaun Standley\*  
 Scott Shaffer\*

Dr. Paul Rosen\*  
 Wendy Edelstein\*  
 Dr. Charles Dunn\*  
 Charles Baker\*

Phillip Barela\*  
 Dr. Yuhsyen Shen\*  
 Ana Maria Guerrero\*  
 Peter Xaypraseuth\*

V Raju Sagi†  
 C V Sreekantha†  
 Nandini Harinath†

Dr. Raj Kumar‡  
 Rakesh Bhan‡  
 C. V. H. S. Sarma†

\*Jet Propulsion Laboratory, California Institute of Technology, 4800 Oak Grove Drive, Pasadena, CA 91109-8099

†Indian Space Research Organisation, U. R. Rao Satellite Centre, Bangalore, 560 017 India

‡Indian Space Research Organisation, Space Applications Centre, Ahmedabad 380015 India

**Abstract**—NISAR is a multi-disciplinary Earth-observing radar mission that makes global measurements of land surface changes that will greatly improve Earth system models. NISAR data will clarify spatially and temporally complex phenomena, including ecosystem disturbances, ice sheet collapse, and natural hazards including earthquakes, tsunamis, volcanoes, and landslides. It provides societally relevant data that will enable better protection of life and property. The mission, a NASA-ISRO partnership, uses two fully polarimetric SARs, one at L-band (L-SAR) and one at S-band (S-SAR), in exact repeating orbits every 12 days that allows interferometric combination of data on repeated passes. NASA provides the L-SAR; a shared deployable reflector; an engineering payload that supports mission-specific data handling, navigation and communication functions; science observation planning and L-SAR data processing. ISRO provides the S-SAR, spacecraft, launch vehicle, satellite operations, and S-SAR data processing. The mission will be launched from the Satish Dhawan Space Centre, Sriharikota, India. Mission development has addressed many unique challenges and incorporates many “firsts” for a jointly-developed free-flyer radar science mission

## 1. MISSION OVERVIEW & CHALLENGES

The imperative to develop NISAR was declared in both the 2007 and 2018 Earth Science Decadal Surveys [1, 2]. The mission is being jointly developed by NASA’s Jet Propulsion Laboratory (JPL) [3] and the Indian Space Research Organisation (ISRO) under an Implementing Arrangement [4] defining responsibilities (Table 1-1). JPL completed a

Critical Design Review in October 2018 and will conduct a System Integration Review in May 2020. ISRO completed Detailed Design Reviews for S-SAR and the satellite in January and November 2019, respectively. NISAR’s target launch is in 2022.

The observatory (Figure 1-1) uses dual frequency, wide-swath, fine resolution multi-polarization L- and S-band SARs with a shared 12-m deployable antenna to make global measurements of land and ice-covered surfaces every 12 days. The spacecraft is ISRO’s high heritage 3-axis stabilized I3K. A JPL-provided engineering payload provides mission-specific needs: GPS for orbit determination; radar data handling; and high-rate downlink system to return mission data. Figure 1-2 shows the mission system architecture. L-SAR data is downlinked via the NASA Near Earth Network (NEN). S-SAR data is downlinked to ISRO stations. The observatory will be launched by ISRO’s Geosynchronous Launch Vehicle (GSLV) Mark 2. The science orbit is 747-km circular, 98° inclination sun-synchronous with a 12-day repeat cycle. Both radars use repeat-pass interferometry requiring exact orbit control within 250 m. The observation plan repeats every 12 days to meet science requirements while balancing energy and downlink capacity. Operations and data processing are jointly performed by ISRO and NASA.

### TABLE OF CONTENTS

1. MISSION OVERVIEW & CHALLENGES.....	1
2. MISSION SCIENCE.....	2
3. SYSTEM ENGINEERING.....	4
4. L-SAR.....	5
5. S-SAR.....	8
6. RADAR ANTENNA & DEPLOYMENT.....	10
7. ENGINEERING PAYLOAD.....	12
8. SPACECRAFT.....	14
9. SYSTEM INTEGRATION AND TEST APPROACH....	16
10. LAUNCH VEHICLE.....	17
11. MISSION OPERATIONS.....	17
12. CONCLUSION.....	19
ACKNOWLEDGEMENTS.....	19
REFERENCES.....	19
BIOGRAPHIES.....	19



Figure 1-1. NISAR Observatory.

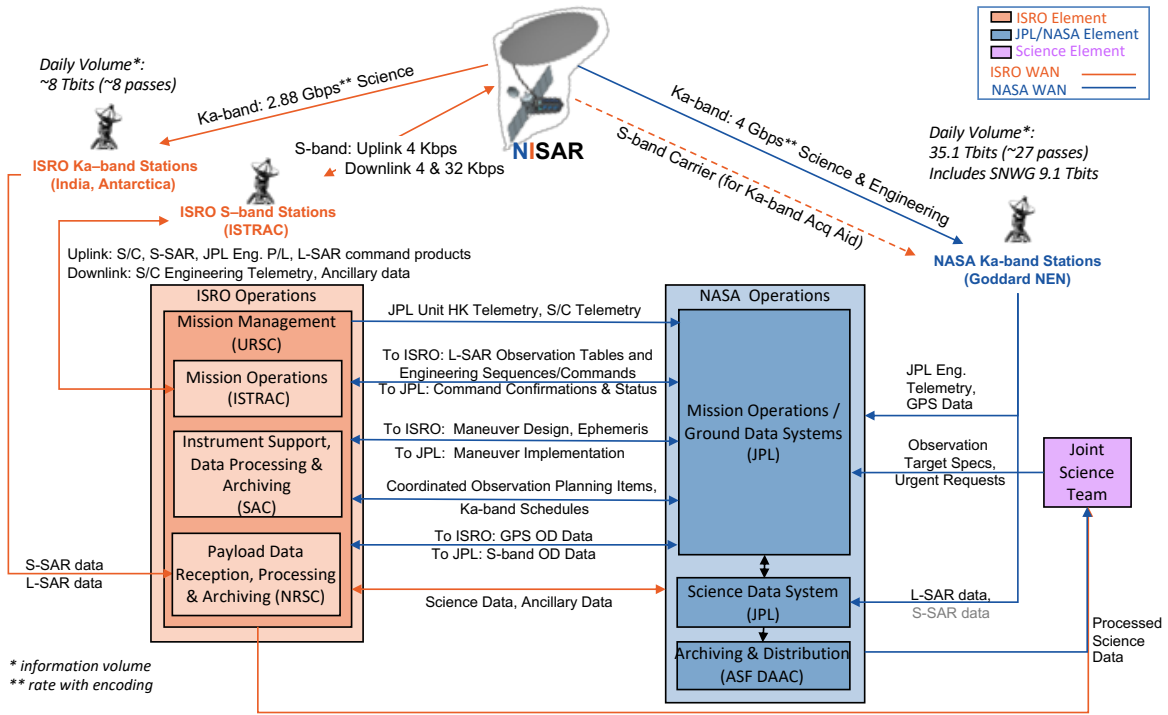


Figure 1-2. NISAR Mission System Architecture.

Table 1-1. NASA and ISRO mission contributions.

NASA Mission Contribution	ISRO Mission Contribution
L-band SAR, shared instrument structure and deployable 12 m reflector and boom assembly	S-band SAR and S-band SAR baseband data handling
Engineering payload (GPS, 14 Tb data recorder and system, NEN-compatible high rate Ka-band system)	Spacecraft mainframe and ISRO-compatible Ka-band high rate communications system; launch vehicle and related services
Integrated radar observation planning and operations	Spacecraft operations, including command uplink and telemetry and tracking
L-SAR data downlink to NASA ground stations	S-SAR, select L-SAR, and spacecraft data downlink to ISRO ground stations
L-band science data processing and distribution	S-band science data processing and distribution

Key challenges addressed by this mission include:

- Very high degree of integration with international partner elements requiring a close coordination between teams separated by 12 time zones and 14,000 km (8700 miles);
- Simultaneous wide-swath, fine resolution, multi-polarization radars providing 12-day global coverage;
- Science observation plan that optimizes measurements while balancing energy and communication constraints;
- Stowing 12-m reflector and boom within a 4-m fairing;
- Accommodating two powerful radars operating at high duty cycle returning 38 Tb/day average data volume;
- On-board handling, downlinking, and timely ground processing and distribution of high daily data volume;
- Precise pointing control for the large, flexible antenna;
- L-SAR waveforms that meet science requirements without interfering with terrestrial navigation systems.

These challenges produced several “firsts,” including:

- High rate direct-to-Earth Ka-band mission data system;
- First digitally beamformed SAR array-fed reflector;
- First dual-frequency SAR using SweepSAR;
- Largest known SAR antenna aperture in history;
- First use of commercial cloud-based ground processing and distribution systems for such a mission;

## 2. MISSION SCIENCE

Science community assessments (2007 and 2018 Decadal Surveys [1, 2] and the NASA Climate Architecture [5]) have identified science questions that are global in scale, fine in resolution, and densely sampled in time, and notably are best or uniquely observed by SAR. Further, SAR is largely unaffected by clouds and can operate at night, making it an excellent utility for applications that require routine and persistent monitoring.

NISAR provides measurements for solid Earth, ecosystems, and cryospheric sciences. For solid Earth, NISAR will characterize long-term and local surface deformation on active faults to model earthquakes and earthquake potential. Faults that move without seismic events are largely unmapped and have a large impact on regional earthquake potential. NISAR enables cataloguing and modeling these faults in regions of high hazard risk. NISAR will acquire systematic deformation measurements over Earth’s many volcanoes to model volcano interiors, forecast eruptions, and map pyroclastic and lahar flows on erupting volcanoes to estimate damage and model future risk. Persistent observations of potential and extant landslides will help to assess and model hazard risk. NISAR will measure subsidence and uplift associated with changes in aquifers and subsurface hydrocarbon reservoirs, which supports characterizing physical and mechanical properties of these bodies and managing their precious resources.

NISAR is well-suited to measuring woody vegetation and soil moisture. For ecosystems, NISAR’s routine observations will better quantify changes in carbon storage and uptake from disturbance and regrowth in dynamic regions. The mission will track changes to active crop extent to aid crop forecasts, and to further quantify the carbon budget. Changes in wetlands extent also affect carbon exchange and will be a target of observations. NISAR will measure freeze/thaw state and permafrost degradation to help close the carbon budget.

A key question is the nature and causes of ice sheet and sea ice changes in relation to atmospheric and ocean forces that act on them, and the relationship of those changes to climate and long-term sea level rise. NISAR will track changes to Greenland’s and Antarctica’s ice sheets, seasonal dynamics of highly mobile and variable sea ice, and inventory variability of mountain glaciers retreating in many places. NISAR will help understand influences of polar atmosphere on snow extent, depth and surface melting—important factors in ice mass balance and cryosphere evolution.

All-weather, day-night, capability is a great advantage for applications that require reliable monitoring, access, and low latency. NISAR has a sensible approach to demonstrate such capabilities. NISAR will be operated to detect, characterize and model potential hazards and disasters on a best effort

basis to demonstrate rapid assessments of urgent events such as earthquakes, volcanic eruptions, floods, and severe storms. These data will support research into effective rescue and recovery activities, system integrity, lifelines, levee stability, urban infrastructure, and environment quality.

These challenging objectives are codified in science requirements (Table 2-1) that are specific in terms of physical parameters—displacements, velocities, biomass, biomass change, and areal extent—and quantified in terms of accuracy, resolution, coverage, sampling, and duration. It is impossible to capture the expansiveness of NISAR’s scientific endeavor in such a set of numbers as they serve to guide the development of this complex and highly capable mission. A full description of the science, measurements, and mission is in the NISAR Science Users’ Handbook [6].

*Measurements*

NISAR’s L-SAR and S-SAR characteristics are in Tables 4-1 and 5-1. Both radars have a 242-km swath enabled by the phased-array-fed-reflector sweep-on-receive design, with selectable polarizations—single, dual, quad, circular, quasi-quad, compact—and a range bandwidths from 5 MHz to 77 MHz. Azimuth resolution is fixed at 7 m which is driven by the antenna size. For solid Earth and most global ecosystems, a 20-MHz dual-pol (horizontal transmit; horizontal and vertical receive) mode is used. Sea ice is observed at 5 MHz with vertical polarization, land ice at 77 MHz with horizontal polarization, and select areas such as North America at 40 MHz with a multi-polarization where a portion of the band is dual pol with horizontal transmit, and the other portion of the band is dual pol with vertical transmit.

NISAR’s repeating orbit cycle allows radar images to be combined interferometrically from one cycle to the next. Interferometric products provide two measurements: (1) a phase difference proportional to ground movement over the interval, with precisions of millimeters to centimeters; and (2) correlation, or “sameness”, of images from one time to the next. Correlation can be used as a proxy for many causes of land surface change, including damage due to shaking, flooding, agricultural activity, and any other processes that can disrupt the surface at the wavelength scale (tens of cm).

**Table 2-1. NISAR top-level science measurement requirements.**

Attribute	2-D Solid Earth Displacement	2-D Ice Sheet and Glacier Displ.	Sea Ice Velocity	Biomass	Disturbance	Cropland, Inundation Area
Resolution	100 m	100 m	5 km grid	100 m (1 ha)	100 m (1 ha)	100 m (1 ha)
Accuracy	3.5 (1+L <sup>1/2</sup> ) mm or better, 0.1 km < L < 50 km, over 70% of areas interest	100 mm or better over 70% of fundamental sampling intervals	100 m/day or better over 70% of areas	20 Mg/Ha for areas of biomass < 100 Mg/ha	80% for areas losing > 50% canopy cover	80% classification accuracy
Sampling	12 days or better, over 80% of all intervals, < 60-day gap over mission	12 days or better	3 days or better	Annual	Annual	12 days or better
Coverage	Land areas predicted to move faster than 1 mm/yr, volcanoes, reservoirs, glacial rebound, landslides	Global ice sheets and glaciers	Arctic and Antarctic Sea Ice	Global areas of woody biomass cover	Global areas of woody biomass cover	Global areas of crops and wetlands

Polarimetric backscatter is used to measure minute geodetic and surface structural changes on a weekly basis. Algorithms map backscatter to biomass and disturbance, and phase and correlation to geodetic displacement and disruption.

*Data Products*

The Project will produce global products up to a level that would be useful as input to a system that creates the final science products (Table 2-2). These products do the bulk of the computational effort, and scientists or value-added organizations can tailor the final products with reasonable effort. Products include complex images at full resolution in both natural radar coordinates and in orthorectified form, and lower resolution polarimetric and interferometric products also in radar and orthorectified coordinates [6].

*Cal/Val Approach*

NISAR uses well-established calibration methods. Corner reflectors placed strategically around the world and with sufficient density will capture expected spatial and temporal variabilities of the radar and measure and validate the image quality through point target signatures. For radiometric balance, the uniform and stable backscatter properties of rain forests in South America and Africa will be used as references. The radars will observe these targets jointly and individually during commissioning and science operations, at first for calibration and validation, and later to check stability.

To calibrate higher-level science products and validate science requirements, an extensive plan is documented in the Science Users’ Handbook and in the Calibration and Validation Plan, both on NISAR’s website. Science algorithms’ calibration uses airborne radar observations from UAVSAR [7], field measurements from GPS for the solid earth and cryosphere requirements, and forest, agricultural, and wetlands measurements for the ecosystems requirements. These are acquired pre-launch to establish relationships needed in the algorithms’ mapping radar measurements to physical measurements. Post-launch, field measurements will validate products against requirements, and other data sets such as lidar forest structure estimates, or Landsat agricultural products will be used for cross-validation.

**3. SYSTEM ENGINEERING**

The observatory consists of a satellite mainframe, a radar instrument payload and engineering payload (Figure 3-1). The satellite mainframe uses the heritage I3K bus to provide power (70V), attitude control, on-board computer (OBC) and command and telemetry (S-band) and mission data communication (Ka-band) to ISRO ground stations using a dual gimballed Ka-band antenna (DGA) that is also shared with the NEN-compatible Ka-band system. The I3K is a standard bus for 3000–3400 kg class satellites and can supply up to 6500 W. The radar instrument payload consists of the L-SAR and S-SAR instruments, a shared instrument structure and a deployable boom and 12-m reflector antenna. The engineering payload provides mission-unique capability for data storage and handling, navigation (GPS), and high rate communication (Ka-band) to NASA NEN stations via the

**Table 2-2. Daily Science Data Product and Volume**

Product	Vol (TB/day)
<b>Level 0</b>	
Incoming Raw Data (to DAAC only)	3.25
Radar Signal Data (RSD)	3.25
<b>Level 1</b>	
Range-Doppler Single-Look Complex	30.33
Multi-Look Detected	0.54
Nearest-Time Interferogram	8.67
Nearest-Time Unwrapped Interferogram	4.33
Polarimetric Covariance Matrix	0.43
<b>Level 2</b>	
Geocoded Single-Look Complex	30.33
Geocoded Unwrapped Interferogram	4.33
Geocoded Polarimetric Covariance Matrix	0.43
<b>Total (TB/day, uncompressed)</b>	<b>85.91</b>

DGA. It includes a 14-Tb solid state recorder (SSR) for radar data storage and a baseband data handler (BDH) to manage S-SAR data transfer and formatting between the S-SAR, SSR, and both Ka-band systems. A payload data system interfaces between the L-SAR and engineering payload and the OBC and provides command and control for JPL elements; it also manages data flow between the radars and Ka-band elements. Orbit ephemeris is provided by a GPS payload. The engineering payload also provides pyro firing signals for the boom and reflector and power distribution and converters to regulate 70V mainframe power to 28V used by JPL Engineering Payload elements.

System requirements were derived from science requirements, opportunities and constraints from heritage elements and existing infrastructure: heritage satellite mainframe, ISRO and NASA Ka-band ground stations (which have different data rates) and the GSLV and 4-m fairing. Other requirements were driven by capabilities’ brought by each mission partner in areas such as operations

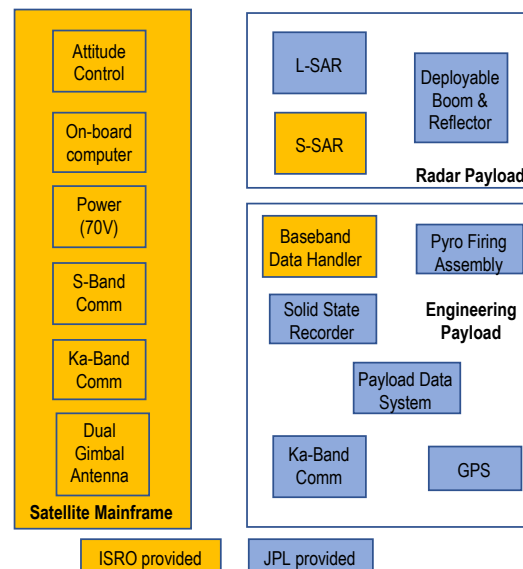


**Figure 3-1. NISAR Observatory System Decomposition.**

and on-board data handling and management. Mass and power allocations are in Table 3-1.

The most challenging mission aspects are the radars which require high power and data capability, and well-controlled pointing. The radars must perform joint and stand-alone observations without interfering with each other. Daily data volumes are allocated to each radar and downlink system. The SSR is a shared resource that must accommodate record, playback and data formatting functions of each radar through different data streams and rates.

Boresight pointing knowledge and stability is driven by SAR image quality (jitter degrades resolution) and geolocation. The  $\pm 10.0$  mdeg (1 sigma) over 3 secs stability is derived from the radar synthetic aperture time, during which signals are combined to achieve the required resolution. This constrains the structural mode frequencies. The observatory must point the antenna relative to geodetic Nadir for radiometric accuracy and relative to the Zero-Doppler Plane to minimize Earth-rotation effects in SAR processing within  $\pm 100.0$  mdeg (1 sigma). For interferometry, the antenna must point to the same target area on repeat passes to  $< 53.6$  mdeg (1 sigma), to reduce geometric and volumetric decorrelation.

Repeat pass interferometry requires orbits to repeat within  $\pm 250$  m of the reference science orbit (RSO) to minimize decorrelation. GPS provides orbit knowledge for precision orbit determination (POD) and data processing. GPS data is included in radar data streams and to the OBC for spacecraft nadir reference. POD reconstructs time to  $\leq 3$   $\mu$ sec relative to GPS Time and orbit position accuracy  $\leq 10$  cm.

Both radars are capable of acquiring data in different configurations with relatively high observation duty cycle (L-SAR 50% and S-SAR 10%) compared to other SAR missions, acquiring a combined average of 38 Tb/day of data.

Radar and engineering payload data are downlinked via a unified Ka-band system to the respective ground stations. An average daily downlink volume of 35 Tb/day will be downlinked to NEN ground stations and 3 Tb/day to ISRO ground stations. Ka-band downlinks utilize dual polarization (right-hand circular and left-hand circular). Switching between downlink paths is accomplished via waveguide transfer switches—one for each polarization—to route RF output to the shared DGA and Ka-band high gain antenna.

Most engineering payload elements are mounted on a mainframe panel (Figure 7-2) while the star-sensors and sun-sensors are mounted on the instrument structure—mounting locations optimize shared-use hardware. The SSR and baseband data handler are also mounted on the instrument structure to keep high rate harnesses short. Star-sensor placement provides radar payload attitudes. Sun-sensor placement minimizes blockage by the radar antenna.

Radar and engineering payload receive mainframe power from the Spacecraft Power Distribution Unit (SPDU) that distributes 70V via relay/fuse feeds. Separate feeds are provided for the payload data handling, L-SAR, S-SAR,

**Table 3-1. Observatory Mass & Operating Power Allocations**

	Mass (kg)	Power (W)
Spacecraft Mainframe	920	1312
Engineering Payload	134	640
L-SAR	283	1515
S-SAR	314	2757
Common Instrument Structure	466	
Reflector and Boom	292	
Propellant	269	
<b>Total</b>	<b>2678</b>	<b>6224</b>

operational heaters, deployment pre-conditioning heaters and survival heaters, with separate feeds for prime and redundant assemblies. JPL elements include power converters to provide regulated 28V. The mainframe power subsystem also provides regulated 70V to mainframe subsystems thru a power distribution unit separated from the SPDU.

Radar interfaces are one-way with cross-strapping between prime and redundant units (Figure 4-3). L-SAR provides the following to S-SAR: 10 MHz reference; transmit synchronization signals; clock; and a serial message indicating L-SAR status. These are required to conduct joint radar observations without interference. L-SAR receives command and control information from the engineering payload data handling subsystem including GPS. Radar data is transferred to the SSR via SerDes. L-SAR provides a radar blanking pulses to GPS during transmit events. L-SAR interfaces are block-configured: prime-to-prime and redundant-to-redundant. S-SAR receives a IPPS signal provided by GPS; other S-SAR interfaces are to mainframe elements (including the high rate SerDes interface with the baseband data handler and the low rate 1553 interface to the OBC). Engineering payload interfaces to the OBC are 1533 for command and telemetry and SerDes to the baseband data handler for S-SAR data write and playback.

The SSR interfaces with the mainframe via the Baseband Data Handler (BDH) that formats S-SAR data to CCSDS telemetry and passes it to the SSR; the BDH also receives data from the SSR for downlink to ISRO ground stations.

## 4. L-SAR

Key radar design drivers include:

- Phased-array-fed reflector to enable wide swath, and fine azimuth resolution drives antenna gain, beamwidth, ISLR, and PSLR performance optimization
- SweepSAR timing, digital beamforming (DBF) to reduce ambiguities and preserve resolution drives signal processing of fast-time varying beamforming coefficients needed to track the angle of the return echo
- Twelve-day global repeat pass interferometry drives:
  - L-band selection to minimize temporal decorrelation
  - Wide swath to ensure coverage at the equator

– High system phase stability requirements

- Polarimetry for classification and biomass drives selection of dual frequency radar
- Split spectrum for ionosphere correction drives flexible waveforms, parallel signal processing at multiple rates
- PRF dithering to fill transmit interference gaps drives the digital control, timing and flight software design
- Urgent response requirement and differing data collection strategies drives seamless mode transitions to prevent data loss at target boundaries
- Wide coverage drives on-board digital filtering and data compression using block floating point quantization to reduce downlink data volume

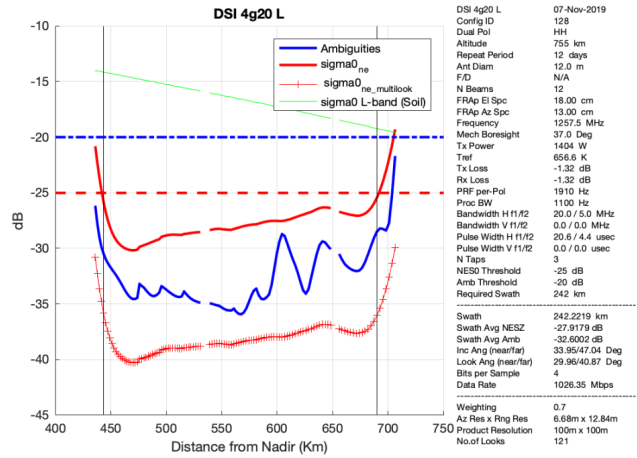


Figure 4-1. L-SAR Sigma0 performance for 20+5 MHz HH mode.

L-SAR driving requirements are in Table 4-1. To achieve the dual-frequency wide-swath data acquisition to meet coverage and revisit requirements, the radars use a shared 12-meter deployable reflector. The reflector is illuminated by a stacked patch array feed that is narrow in the along-track direction and wide in the cross-track direction to produce a fan-beam illumination pattern. On transmit, the entire swath is illuminated. On receive, echo signals from each set of radiating elements in the cross-track direction are received and digitized independently to allow formation of several simultaneous receive beams across the swath. The beams are combined on receive using fast time varying weights to track the peak return energy in the echo as it sweeps across the swath from the near to far range. This technique (SweepSAR) was demonstrated in airborne experiments [8]. NISAR is the first space-based dual-frequency SAR to use this technique. Representative simulated performance for the most commonly used L-SAR 20+5 MHz HH mode is shown in Figure 4-1, showing Noise-Equivalent Sigma-Naught and ambiguities meet requirements over the full 242 km swath.

*Design, Key Trades, and Challenges*

The radar configuration is in Figure 4-2. An octagonal aluminum structure houses both L- and S-SAR and the shared 12-m reflector and 8.5-m boom stow around the structure for launch. Electronics are mounted internally and externally to efficiently accommodate the radars, their separate feeds, and reflector and boom in stowed and deployed configurations.

L-SAR uses an RF back-end (RBE), 24 transmit/receive modules (TRMs), H- and V-pol digital electronics, redundant radar instrument controllers (RIC), 6-quad first stage processors (QFSPs), and 2-second stage processors (SSPs). The instrument structure houses harnesses, thermal hardware and reflector/boom launch tiedowns. The configuration optimizes mass, structural and thermal robustness, and I&T considerations. The structure has removable panels to mount internal electronics and a removable 3-sided “clamshell” for the S-SAR; the clamshell is provided to ISRO to integrate and test the S-SAR and deliver the integrated unit to JPL for radar payload I&T. L-SAR signal processors and TRMs are

Table 4-1. L-SAR Driving Radar Requirements.

Functional Requirements	Parameter
Operating Frequency	1219.0–1296.0 MHz
RF Transmit Power	1400 w Peak per pol, 120 W per T/R module
Antenna type	12 m array-fed deployable mesh reflector
Number of beams	12 beams
Revisit time	12 days
Resolution	3-10 m
Polarization	HH and VV, HH/HV and VV/VH, QP, QQP
Bandwidths	5 MHz, 20 MHz, 40 MHz, 77 MHz, 20/5 MHz split spectrum, 40/5 split spectrum
Pulsewidths	10 us, 20 us, 25 us, 40 us, 45 us
Pulse Repetition Frequency (PRF)	1000 Hz–4000 Hz
Block Floating Point Quantization (BFPQ)	16 to 3, 4, or 8 bits
Data Rate (to SSR)	3.84 Gb/s
Radar Electronics DC Power	1515 W peak during data take
Radar Electronics Mass	283 Kg
Radar Antenna Mass (boom, reflector, feed)	292 Kg
Structure Mass (common instrument structure, thermal hardware and system harness)	466 Kg
Performance Requirements	Parameter
Signal to Noise Ratio (SNR)	>-15 dB in quad-pol mode >-20 dB for all other modes
Radiometric accuracy	<0.75 dB (co-pol) <0.90 dB (cross-pol)
Systematic phase accuracy	<3 deg
Antenna pointing knowledge	<39 mdeg

mounted externally with thermal radiators built into covers. The L-SAR RF backend, control electronics and all S-SAR electronics are inside the structure with external thermal

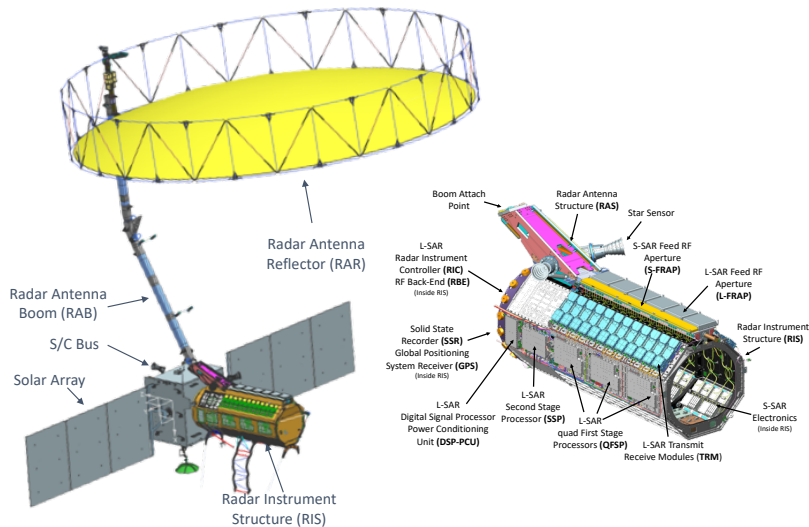


Figure 4-2. L-SAR Flight-deployed configuration.

radiators. Mounting L-SAR electronics externally allows for efficient thermal radiator fields-of-view, but it also requires additional packaging attention and mass to reduce micrometeoroid damage risk.

The L-SAR block diagram is in Figure 4-3 including interfaces to the S-SAR, Engineering Payload and Spacecraft. The radar backend generates clock/timing signals, chirp waveforms and upconverts them to L-band. A transmit beamformer distributes chirps to 12 H-pol and 12 V-pol TRMs. Each TRM amplifies transmit waveforms to 120 W RF power and provides low noise amplification for returned echoes. Each TRMs has calibration loops that route

transmit and receive chirps, and calibration tones. Return echoes are digitized by 12-bit analog-to-digital converters in the QFSPs, that also perform digital filtering and calibration coefficient estimation. The SSP completes digital beamforming (DBF) and reduces data using a Block Floating Point Quantizer. The radar controller uses a RAD750 flight computer for command and telemetry and has a SerDes SSR interface.

The system is designed to be fully polarimetric, including both H and V transmit channels and receive channels, resulting in four fully polarimetric signatures (HH, HV, VH, VV) of the target. If one of the two transmit polarization channels fail or one of two receive polarization channels fail, the system still is capable of meeting its science requirements.

Spaceborne L-band active remote sensing radars share bands used by terrestrial navigation radars and GPS; consequently, licensing involves analysis to ensure no interference by orbiting radars to terrestrial systems. The NTIA Stage 3 review process necessitated changes to the L-SAR waveforms to avoid operational restrictions. Revised waveforms now meet science needs and are expected to get NTIA Stage 4 approval without restrictions.

SweepSAR DBF uses channel-relative calibrations to avoid SNR degradation. Each echo is sampled, filtered, beamformed, further filtered, and compressed on board. Because

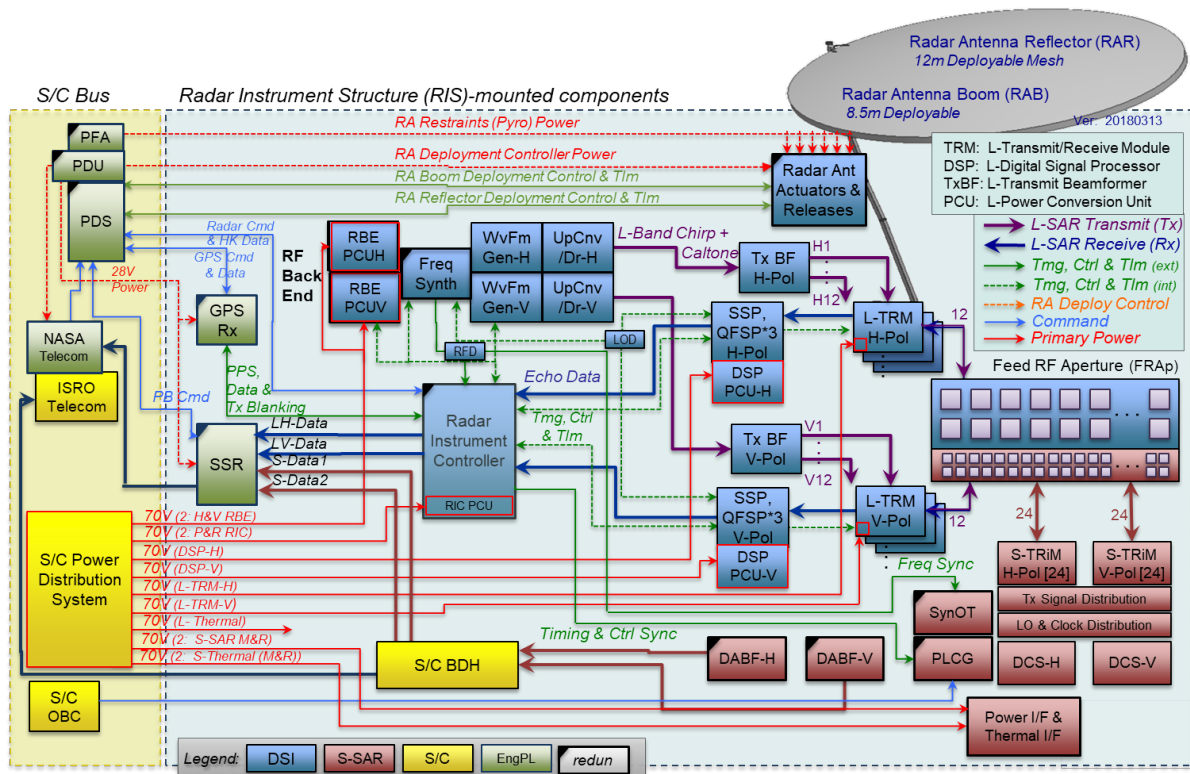


Figure 4-3. L-SAR Block Diagram with Interfaces to S-SAR, Engineering Payload, and Satellite Mainframe

channels are summed before downlink, the process is not reversible on the ground. Extensive ground testing of calibration algorithms ensures this works over all conditions.

SweepSAR using a large reflector and active array feed poses two challenges to V&V: 1) the antenna’s size prevents pattern measurement and 2) the wide thermal variation from reasonable beta angle changes. It is impractical to measure patterns in its deployed configuration in a thermally-controlled environment. These two challenges are being addressed by the following steps: (a) performing measurements of the feed antenna patterns, in ambient, with and without TRMs, (b) building a verifiable structure, thermal and electromagnetic performance (STEP) model of the mechanical structures, including a thermally-distorted radar antenna, and (c) combining the thermally-tested TRMs, the measured feed patterns, the STEP-provided geometry distortion with antenna RF modeling tools to predict the radar antenna patterns in the on-orbit thermal environment. Post-launch, point targets and natural homogeneous targets will be used to resolve any antenna pattern errors after deployment.

For end-to-end calibration, NISAR uses built-in internal calibration to track electronics’ temporal short-term drift and ground calibration sites as external calibration to improve accuracy. Internal calibration routes signals through each TRM, and the calibration signals are detected in flight or can be ground extracted to calibrate system short-term variations. External calibrations (using data acquired over instrumented calibration sites and homogeneous extended sites) enables absolute radiometric calibration and antenna pointing calibration. If necessary, onboard tables that control on-board radar signal processing can be updated to optimize radar performance.

*I&T, V&V, and Calibration*

L-SAR is being integrated at JPL (Figure 4-4) and includes full radar performance tests to verify the system—a challenge due to 24 separate channels that must each be tested over polarizations, pulse widths, bandwidths and center frequencies, each with different calibration corrections. L-SAR supports 64 stand-alone and 64 joint configurations; however, science operations has only identified 19 L-SAR and 19 joint L-SAR/S-SAR configurations for use in flight, simplifying testing. L-SAR will undergo thermal vacuum test to perform pre-launch calibrations and verify that radar



**Figure 4-4. L-SAR in integration and test at JPL**

performance is stable and repeatable. This occurs without the feed tiles so that transmit and receive channels and calibration paths can be characterized over temperature using a target simulator. L-SAR has an internal cal loop to characterize transmit power, receiver gain, quantization noise, and phase stability and to adjust the calibration and beamforming coefficients for changes in performance. Calibration coefficients will be verified over temperature and corrected to remove temperature dependent changes outside the cal loop. On-orbit, data takes consist of a pre-take, observations, and a post-take. The radar performs an automatic internal calibration sequence during the pre- and post-takes and uses these coefficients to calibrate the system.

**5. S-SAR**

S-SAR provides single, dual, compact and quasi-quad polarization imaging modes. The system design, configuration, realization and testing is challenging because both L- and S-SARs operate at the same PRF during joint operation. SweepSAR requires dithering to avoid gaps in the swath from receive echo conflicts with transmit events. ISRO will use a Portable 1-D antenna test facility for in-situ calibrations of the 24 element array feed along with radar hardware. ISRO also plans an airborne L- and S-SAR system (DFSS) to deliver NISAR-analogue data products to the science community.

S-SAR uses the SweepSAR technique [9]; key specifications are in Table 5-1. S-SAR also uses DBF on receive to enable wide swath measurements, very high resolution (5–10 m) and repeat pass interferometry [10, 11]. Until now, large swath imaging by SAR is achieved by compromising on resolution to the order of 50 m. S-SAR is configured for multi-polarization and is capable of providing polarimetric data. A key advantage of the reflector configuration is it requires a small number of TRMs (e.g., 24 pairs compared with ~160 pairs for an active antenna-based SAR); however, each TRM has a higher transmit power. Payload operation has been defined per the application needs which include targets across globe.

*System Design and Configuration*

S-SAR operates in the 3100–3300 MHz band allocated for earth-exploration satellites (active). To meet science and applications requirements defined in Table 5-1, S-SAR includes Single/Dual/Compact/Quasi-Quad polarization. The configuration includes an active-array 24 × 2 array feed in the

**Table 5-1. Major Specifications of S-band SAR of NISAR.**

Orbit	747 km with 98° inclination
Frequency	3.2 GHz
Repeat Cycle	12 days
Roll Bias	37°
Incidence Angle Coverage	33° to 48°
Primary Feed Antenna	2 m Active Array
Secondary Antenna	12 m Diameter Reflector
Sigma naught	–20 dB
Resolution	6 m (Range and Azimuth)

focal plane of the reflector. The long array dimension is in elevation to enable beam scanning. Antenna feed patches are dual polarized, fed by a dedicated pair of TRMs (H+V), thereby, necessitating 24 pairs for H & V polarizations.

S-SAR electronics include TRMs, a controller and digital chirp generator, synchronized oscillator and central transmitter, data acquisition and beam former systems and distribution networks for transmit signal, local oscillator and clock. Electronics are mounted on a JPL provided “clamshell.” TRM outputs connect to the antenna through 2.5 m coax RF cables; lengths are kept equal to maintain equi-phase relation across the feed. To meet Noise-Equivalent Sigma-naught (NESZ) requirements with the imaging geometry and antenna, a peak transmit power of 3960W is needed, which translates to 165 W per TRM. Different modes have been identified to meet the science requirements. Various polarization combinations, chirp bandwidths of 10, 25, 37.5, and 75 MHz, nominal pulsewidth of 25  $\mu$ s (10  $\mu$ s for joint mode) and nominal PRF of 2200 Hz (1910 Hz for joint modes) are used.

### Imaging Geometry

For global coverage and repeatability, the reflector boresight is at 37°. The feed-array length and TRMs (and hence, number of receive beams) have been fixed to produce an incidence-angle span of 32.9° to 47.9°, which corresponds to off-nadir distance of 425 km to 699 km respectively, to produce a 242 km swath. The feed-structure and reflector geometry maximizes reflector illumination in receive-mode. To achieve a look angle of 37°, the spacecraft is roll-tilted by 16.33° (Figure 5-1).

S- and L-band feed-arrays are side-by-side in azimuth causing a squint of +0.35° and -0.9° respectively, that create non-zero Doppler centroids. During imaging, yaw-steering the spacecraft to compensate for Earth Doppler will be done considering a mean/ intermediate reference squint angle, therefore, it will not fully compensate the Doppler due to squint and has to be corrected during ground data processing.

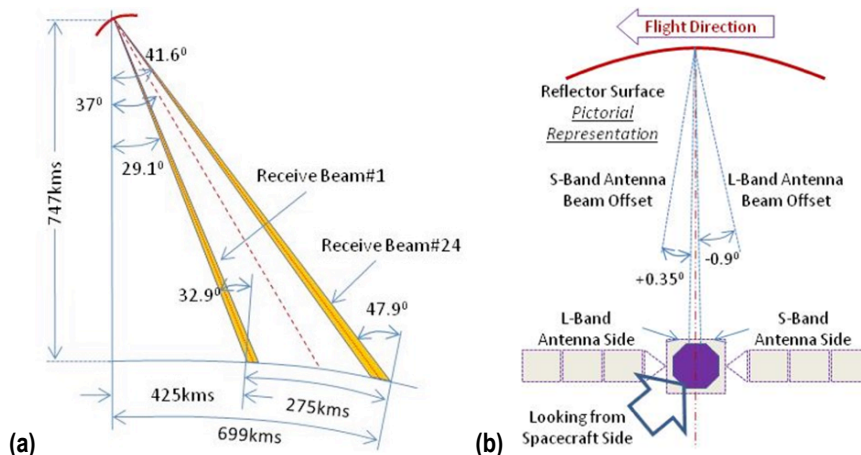


Figure 5-1. S-SAR Imaging geometry (a) elevation (b) azimuth.

### S-SAR Operation Modes

Six operation modes are defined to meet science requirements. Operational bandwidth for each mode varies per target resolution requirement. In Compact Polarization combination, referred to as CP in Table 5-2, H & V polarizations are transmitted simultaneously with a relative phase difference of 90°. The main advantages of this mode is (i) polarimetry without compromising swath or data-rates; (ii) self-calibrating in nature, estimation of phase-difference between H & V channels and subsequent correction is possible; (iii) little impact of Faraday rotation from ionosphere propagation.

Table 5-2. Science Requirements of S-SAR & dual freq modes.

Science Target	Operation Polarization
Polarization	HH, HV, VV, VH, HH+HV+VV+VH
Solid Earth /Ice/Veg/ Coast/ Bathymetry	Quasi-Quad Polarization (QQP)
Ecosystem/ Coastal Ocean/ Cryosphere	DP(HH/HV) or(VV/VH)
Agriculture /Sea Ice	CP RH/RV
Glacial Ice – High Resolution	CP RH/RV
Deformation	SP HH (or SP VV)
Deformation – Max Resolution	SP HH (or SP VV)
Glacial Ice – Himalayas	L: DP HH/HV and S: CP RH/RV
Sea Ice Types	L: DP VV/VH and S: CP RH/RV
India Agriculture	L: QP HH/HV/VH/VV and S: CP RH/RV
High-Res Deformation	L: DP HH/HV and S: SP HH (or SPVV)

SAR performance has been simulated for Noise-Equivalent Sigma Naught ( $NE\sigma_0$ ) and ambiguities in Figure 5-2. Because of the wide swath, receive power across different channels is analyzed for dynamic power variation. Uniform  $NE\sigma_0$  of -20 dB results in -88dBm receive-power and lower limit will be noise-floor corresponding to different bandwidths. Considering -10dB as maximum sigma naught, -78 dBm will be the maximum receive-power.

On transmit, all TRMs radiate simultaneously producing a narrow aperture illumination (~0.6 m) in elevation, but full 12-m in azimuth. This produces the 240 km swath over the imaging region. On receive, TRMs are activated one-at-a-time, thereby, maximizing receive-aperture to full 12 m. This results in higher gain of the ground-return signal, but narrow footprint on the imaging region. The pointing angle of the secondary beam depends on the position of the receiving-patch on the feed-structure. As the location of the patches is linearly distributed in elevation, the 24 TRMs result in 24 receive-beams spanning the

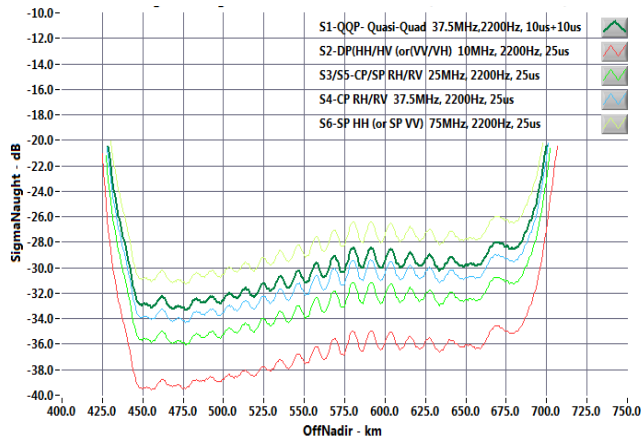


Figure 5-2. SigmaNaught profile for different science modes.

entire swath which is coincident with the wide-footprint of transmit-beam.

### Receive Channel Phase Imbalance

An active array antenna must maintain a constant phase front at boresight. All RF electrical path lengths including active and passive elements up to the antenna radiating elements must be equal, so that insertion phase and gain of the signal reaching to each element is equal. During fabrication of RF electronics and distributed integration elements including RF cables and corporate feed networks, mismatch of gain and phase is introduced so that the phase front of the active array may randomly deviate. This results in disruption of collimation of phased array antenna.

Various methods like frequency domain method, zero crossings method, time domain multiplication method were studied and simulated for delay estimation. After comparing the results and considering the requirement, time domain multiplication method was selected for estimation of delay across receive channels (Figure 5-3).

## 6. RADAR ANTENNA & DEPLOYMENT

The radar antenna consists of L- and S-SAR feed arrays and the deployable boom and reflector. Accommodating the reflector and boom within a 4-m fairing drives a stowed configuration that wraps around the structure (Figure 6-1).

The antenna optical prescription defines key geometrical relationships, particularly the reflector size and curvature and its orientation to the feed; key requirements are in Table 6-1.

The L-SAR feed is a linear array of six tiles, each as a pair of dual-polarized patch antennas (Figure 6-2). Each pair is differentially-fed in elevation for v-pol and in azimuth for h-pol. The tiles are thermally-controlled for phase stability by a polyimide-filled Astroquartz radome with a white-painted shell and rear-mounted strip heaters.

A dimensionally stable composite honeycomb antenna support structure provides a stable mechanical reference for the feed tiles and boom interface (Figure 6-3). It is pseudo-

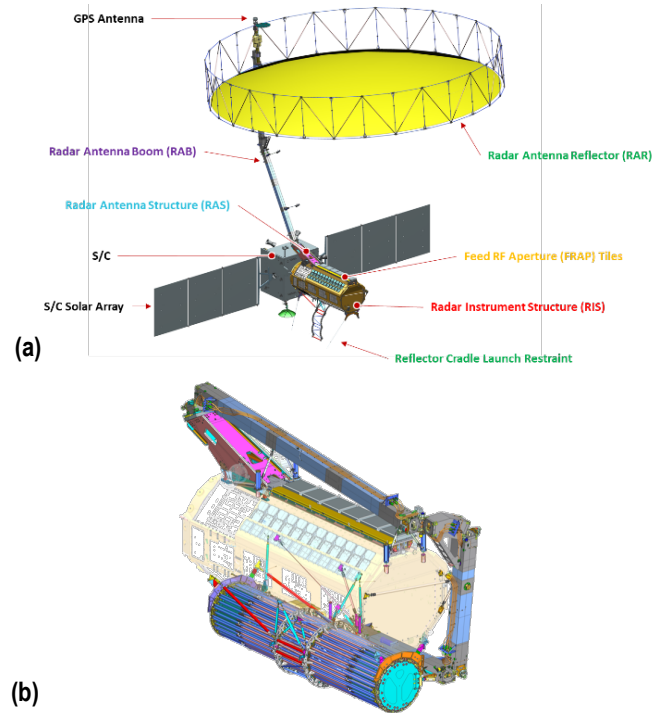


Figure 6-1. Radar Antenna in (a) Deployed and (b) Stowed configurations.

kinematically mounted at the in-board end and cantilevered in order to eliminate distortions from the aluminum instrument structure. The outboard end is restrained at launch to increase stiffness and reduce deflections.

The boom maintains the focal length between feed tiles and reflector and consists of 7" square composite tubes, 8.5 meters long with four hinges (Figure 6-4). The structure and hinges are designed for ultra-high stability over large temperature variations. The hinges use springs and dampers to deploy and an actuator-driven latch to preload the closed hinge on four cup-cones for a repeatable and stiff joint.

The reflector is an Astromesh AM-1 design developed by Northrup Grumman Astro (Figure 6-5). The antenna has a perimeter truss with a reflecting surface of gold-coated

Table 6-1. Key Antenna Requirements

Key Requirement	Description	
	L-band	S-band
Antenna Type	Offset-fed deployable parabolic reflector	
Projected aperture	12 meters	
Focal length	9 meters (f/D = 0.75)	
Antenna Gain	39 dB	42 dB
Gain Stability	<0.01 dB	<0.02 dB
Sidelobe level (at nadir)	-45 dB	
Integrated Cross Pol	-18 dB	
Beamwidth	<1.4°	<0.7°
Reflector surface	10 OPI*, gold-plated molybdenum mesh	
Feed type	Phased-array (6 el)	Phased-array (6 el)

\*openings per inch

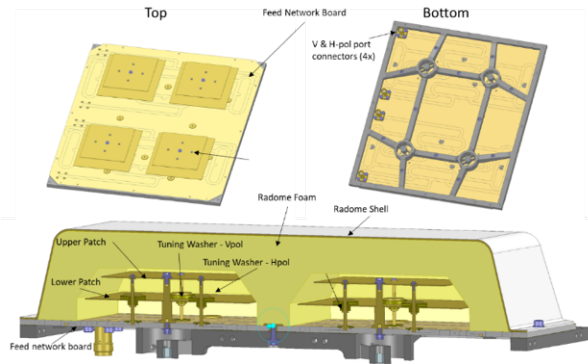


**Figure 6-2. L-band Feed Tile configuration.**



**Figure 6-3. Antenna Support structure.**

molybdenum mesh. The reflector stows into a cylindrical bundle held by a cradle. It has a set of four launch restraints.

The reflector is deployed shortly after launch over six days (Figure 6-6). Initially, heaters warm the instrument structure to relieve thermo-elastic loads between aluminum and composite elements. Deployment begins by releasing the antenna support structure, boom and reflector launch restraints. During deployment, attitude control is open-loop to avoid control forces. Limited real time telemetry is available via S-band. After each deployment step, complete telemetry is sent via Ka-band for evaluation. Deployment telemetry includes limit switches for hinge closure and latching; potentiometers to confirm hinge angle; motor currents; and bus inertial measurements.

Before reflector deployment, a rotisserie maneuver about the boom axis thermally equilibrates the stowed reflector. A momentum bias is applied to reduce off-sun drift. Reflector deployment occurs in two phases: a passive “bloom” and a powered deployment. Tension sensors are monitored by engineering payload software during the powered phase to power off motors when deployment is complete.

Antenna development overcame several challenges. An iterative offset design led to a partially blocked aperture compromise that minimized radar ambiguities, improved cross-pol isolation, and maximized signal-to-noise ratio. Boom stowage traded tube geometric complexity and number of hinges. The “wrap-around” configuration and launch restraints over-constrained the system but reduced launch loads to reasonable levels. Seventeen degrees of freedom are constrained by five launch constraints and interfaces to the antenna support structure and reflector. Modeling later showed over-constraints caused large thermo-elastic loads



**Figure 6-4. Boom segments being assembled at JPL.**

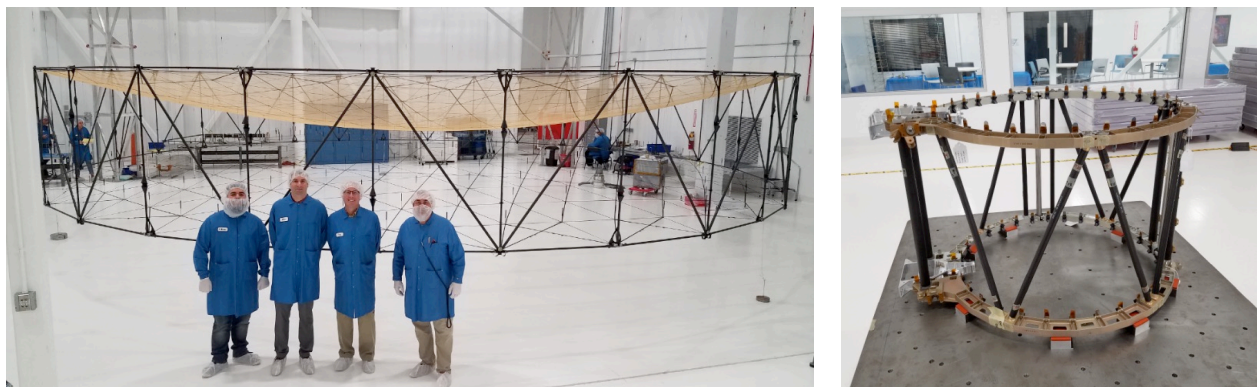


**Figure 6-5. Perimeter Truss with Mesh Reflector Surface in Assembly; Cradle Launch Restraint.**

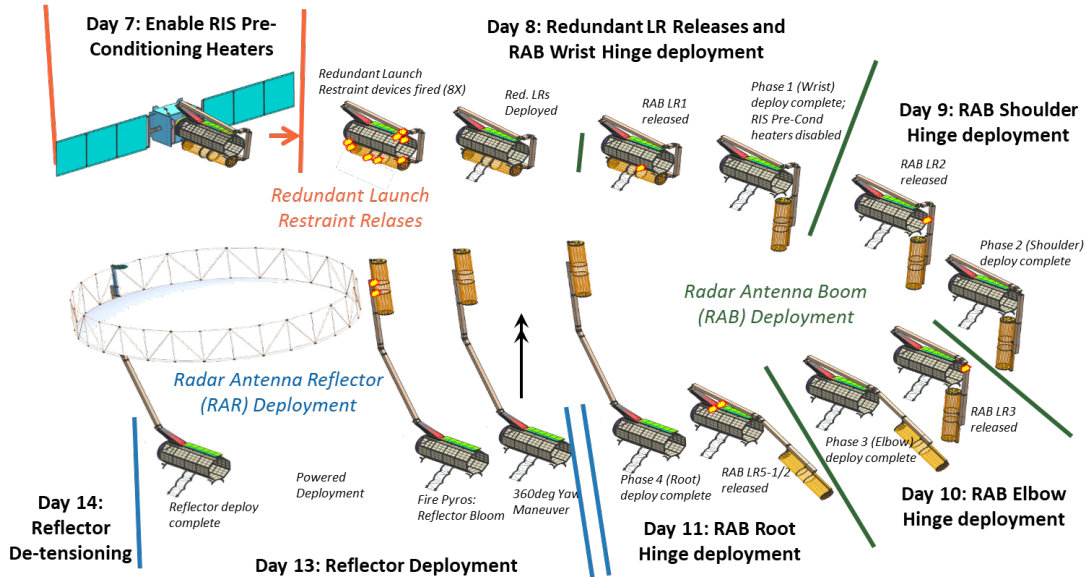


Figure 6-6. Radar Antenna Deployment Overview.

(comparable to launch loads) on the stowed boom and reflector from large thermally-induced dimensional changes between aluminum and composite structures. An expanded test program added additional coupon thermal cycling to increase temperature allowables. Later, thermo-elastic loads were found to cause bolt entrapment risk during cradle release. This was resolved by adding pre-conditioning heaters to the aluminum structure to reduce thermo-elastic loads before deployment. Additional changes were made to lower entrapment risk followed by testing a mock up to demonstrate that entrapment would not occur under worst-case conditions.

## 7. ENGINEERING PAYLOAD

The Engineering Payload block diagram is in Figure 7-1; it includes the Payload Data System, SSR, GPS Payload (receivers and antenna), Payload Communication System

(PCS), and Power Distribution and Pyro Firing Assembly (PFA). Functions and interfaces are redundant; resources are in Table 7-1. Most elements mount on a mainframe panel (Figure 7-2). The SSR and GPSP mount on the instrument.

Engineering Payload is largely block redundant. Exceptions are the GPS antenna, which is switched between redundant receivers, the PFA, which is internally redundant and cross-strapped between the Engineering Payload blocks and the PCS and the SSR whose redundancy are described below.

Table 7-1. Mass and power for Engineering payload.

EP Element	Mass (kg)	Power (W)
Payload Data system	19.7	55.0
Solid State Recorder	26.8	135.0
GPS Payload	17.1	34.1
Payload Comm System	17.7	175.0
Power Distribution Unit	15.8	106.0
Pyro Firing Assembly	10.8	
Harnessing, other items	26.1	
<b>Total</b>	<b>134.0</b>	<b>640.0</b>

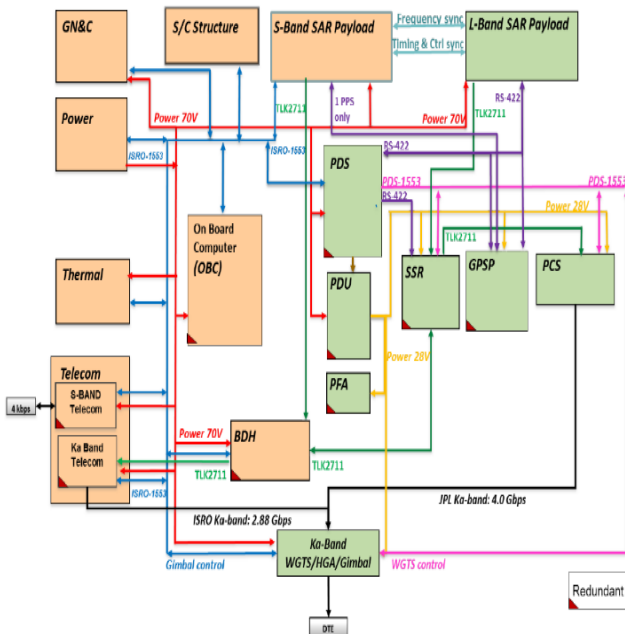


Figure 7-1. Engineering Payload high level block diagram.

### Payload Data System (PDS)

The PDS provides command and control functions for JPL elements, including boom and reflector deployments, power switching, data management, telemetry collection, NASA/JPL Ka-band downlink configuration and fault management. Commands and attitude data are received from the mainframe OBC via 1553 and are routed to other elements via 1553 and 422 interfaces. The PDS receives telemetry from JPL elements and passes health and fault status to the OBC. It consists of two block-redundant, cold-spares boxes, each with seven boards on a PCI backplane. It uses a BAE RAD750 with JPL flight software. The PDS is based on the SMAP Command and Data Handling design.

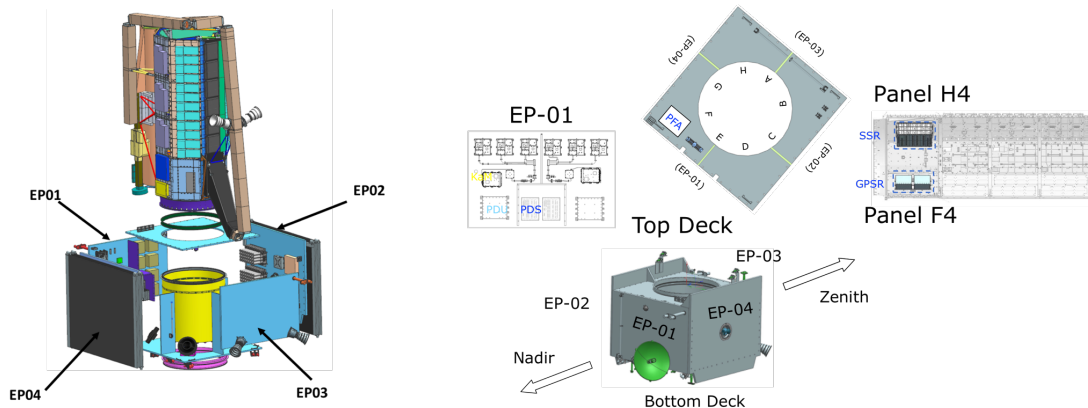


Figure 7-2. Engineering Payload Element Mounting Locations on NISAR Observatory.



Figure 7-3. Payload Data System.



Figure 7-4. Solid State Recorder.

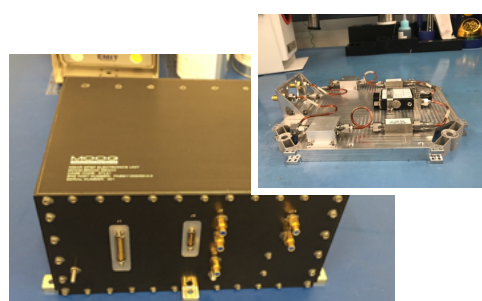


Figure 7-5. GPS receiver and BPF/LNA/Switch Plate.

### Solid State Recorder (SSR)

An Airbus-developed 14 Tb SSR acquires, records, stores, protects, plays back, formats and transmits data received from the SARs. It is internally redundant with cross strapped external interfaces. It receives science data and telemetry directly from the L-SAR via two 1.92 Gbps Serializer/Deserializer (SerDes) interfaces. The S-SAR data interface to the SSR and PCS is mediated by ISRO's Baseband Data Handler (BDH). S-SAR data is provided on four 1.28 Gbps SerDes interfaces. Playback is controlled by the PDS. The SSR performs formatting and encoding of playback data and supports real time downlink of engineering data.

### Global Position System (GPS) Payload (GPSP)

GPSP has redundant GPS receivers developed by MOOG-Broadreach (Cosmic-2 heritage); and one antenna with bandpass filter, low noise amplifiers and a redundancy switch located at outboard boom tip for field of view. GPSP provides

standard time for NISAR, a 1 pps signal to the OBC, L- and S-SAR for synchronization and time correlation, and ephemeris data for science processing and orbit determination. GPSP receives blanking pulses from L-SAR controller to protect its receiver.

The antenna location was evaluated for multipath and boom deployment errors that could degrade orbit-to-orbit position differences critical to interferometry. Multipath can be partially mitigated by developing empirical models of multipath from inflight data. Analysis determined that at 750 km altitude, one GPS antenna atop of the Radar reflector produces an average 3D position error < 10 cm (1-sigma) and average velocity error < 0.1 mm/s (1-sigma). The position accuracy meets the 20 m per axis requirement [12].

### Payload Communication System (PCS)

PCS provides high-rate downlink (2 Gb/sec coded, averaging 35 Tb/day) L-SAR data to the NEN. It is dual polarization with parallel Ka-band chains operating at ~1.74 Gbps per channel. Each chain uses a Ka-Modulator (KaM), a QuinStar solid state power amplifier (SSPA, 1 W), a bandpass filter and waveguide transfer switch between ISRO and JPL systems (Figure 7-7). The PCS uses a shared ISRO 70-cm mainframe antenna with two-axis steering commanded by the OBC that supports left and right circular polarization with 41 dBi gain. The PCS is functionally redundant; observatory layout is shown in Figure 7-8.

The JPL-developed KaM (Figure 7-9) is based on earlier software-defined radios with uploadable software and firmware (Electra). It transmits in the near-Earth band (25.5–

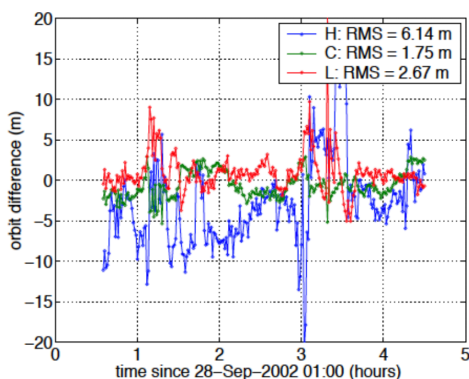


Figure 7-6. GPS Multipath-Induced On-orbit Errors [12].

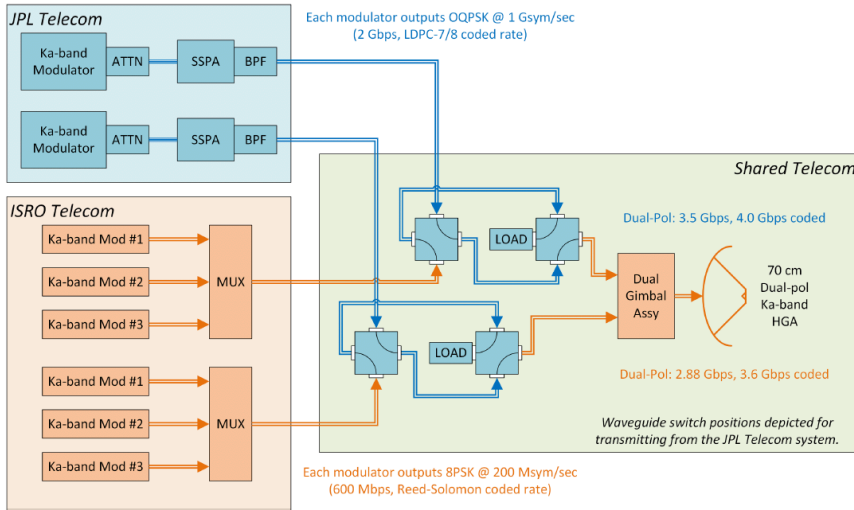


Figure 7-7. PCS block diagram.



Figure 7-9. Ka-band Modulator.

comply with NASA-STD-8715.7 requirements for range and payload safety. The PFA is derived from JPL designs developed for the MSL and SMAP missions.

## 8. SPACECRAFT

### Spacecraft Mainframe Design

The mainframe meets mission needs with heritage designs and interfaces from previous ISRO spacecraft. The stowed configuration is in Figure 8-1; deployed in Figure 8-2. Figure 8-3 is the system block diagram. Resources are in Table 8-1.

**Structure**—The structure is based on I3k spacecraft, which uses a flight-proven cuboid with central cylinder. The cuboid is 1.9×1.8×1.2 m and encloses a central cylinder 1.2 m dia that extends above the top deck with metallic rings at each end. The aft ring interfaces with the launch adaptor and supports the bottom deck; the forward ring is the payload interface. Four vertical decks are supported by shear webs attached to the cylinder. The shear webs are composite-aluminum honeycomb sandwich; all cuboid decks are metallic sandwich construction.

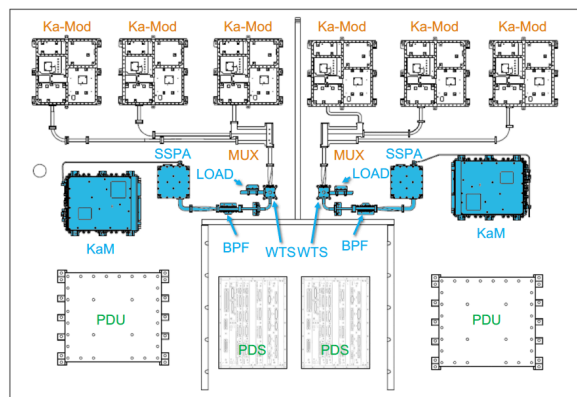
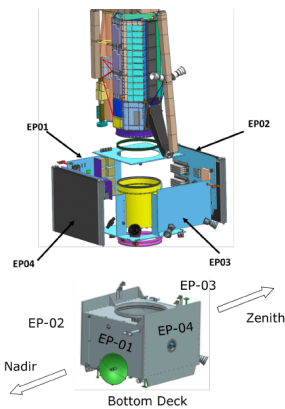


Figure 7-8. PCS layout on EP-01 panel (items shaded in blue are JPL PCS deliverables).

27 GHz) at coded rates of 500, 1000, 2000 Msps. It supports offset quadrature phase shift keying with root raised cosine pulse shaping, baseband filtering, and low density parity check modulation at rate 223/255 with AOS frame alignment.

### Power Distribution Unit (PDU)

The JPL-developed PDU converts 70V mainframe voltage to 28V regulated for use by Engineering Payload elements. It provides switched 70V to 70V switched power for the PFA.

### Pyro Firing Assembly (PFA)

The JPL-developed PFA provides 18 redundant (18 × 2) output drivers capable of driving two simultaneous pyros firing signals for both non-explosive actuators and NASA standard initiators. It includes inhibits to

ring interfaces with the launch adaptor and supports the bottom deck; the forward ring is the payload interface. Four vertical decks are supported by shear webs attached to the cylinder. The shear webs are composite-aluminum honeycomb sandwich; all cuboid decks are metallic sandwich construction.

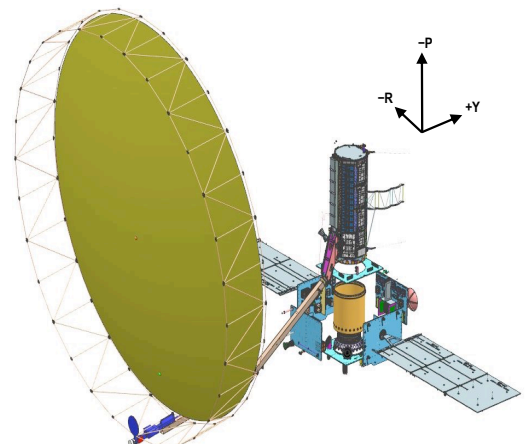
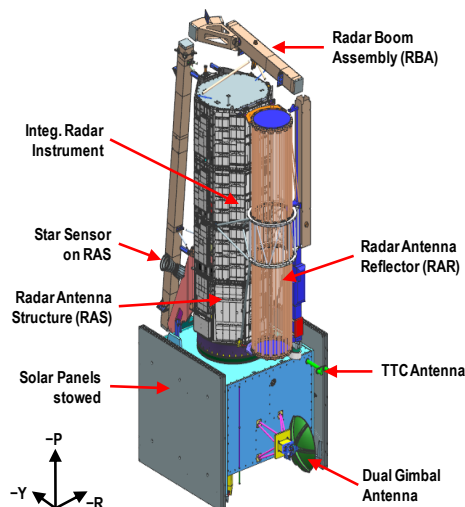


Figure 8-1. Observatory stowed configuration. Figure 8-2. Observatory deployed configuration.

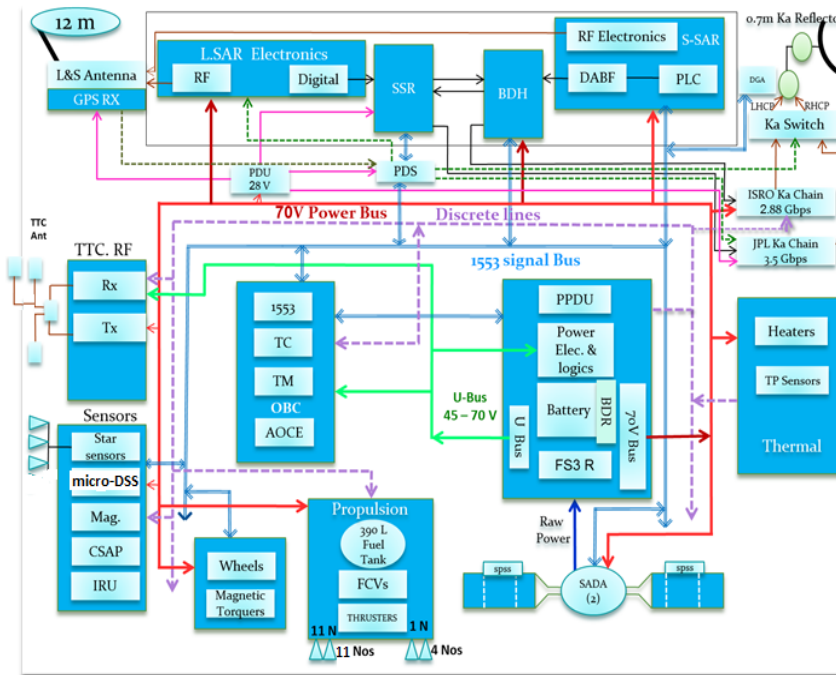


Figure 8-3. Spacecraft Mainframe System Block.

Table 8-1. Mainframe System Mass and Power Allocations.

Subsystem	Mass (kg)	Power (W)
Mainframe System	919.6	1312.3
Structure and Thermal	209.2	320.0
Propulsion	47.3	—
OBC	66.2	110.5
ACS Sensors and IRU	120.8	354
Power	247.9	175
S-, Ka-, and BDH	51.8	235
AIT Elements	132.4	50
Mechanism	44.0	67.8

**Attitude Control System (ACS)**—ACS is zero momentum bias with software on the OBCs that draws heritage from LEO missions. Reaction control uses wheels and magnetic torquers. Sensors include star and sun sensors, inertial reference units (IRUs) and an accelerometer package. Four 50 Nms wheels mounted in a tetrahedral provide fault tolerance. Three torquers (565 and 350 Am<sup>2</sup>) continuously dump momentum. Wheels are sized for orbit maintenance maneuvers and thermal gradients during deployments.

The propulsion system thrusters are block redundant with a 390L propellant tank (surface tension type) connected to the blocks through single flow path latch valves and filters. One thruster block can perform all attitude and orbit control maneuvers required by the mission. The system uses ten 11 N thrusters (canted), one central 11 N thruster on the pitch axis and four 1 N thrusters on roll axis. The propellant load is 260 kg.

Redundant IRUs in the three spacecraft axes provide increment angle for attitude reference. IRUs use three dry-tuned gyros (DTGs) in roll, pitch, and yaw axes in

orthogonal configuration. DTGs are mounted in a vibration-isolated cluster. DTGs are thermal-controlled for stable performance.

A Ceramic Servo Accelerometer Package (CSAP) measures incremental velocity along roll, pitch and yaw axes. It is used to terminate thruster firing when the required  $\Delta V$  is achieved during orbit maneuvers. It provides  $\Delta V$  accuracy of 0.1%.

Mark III star sensors with an accuracy of 10 arcsec across the bore site axis use CMOS detectors with Peltier coolers. Sensors can tolerate sun intrusion while powered off for more than 20 minutes.

**Power System**—The spacecraft uses a single regulated 70V power bus, sized for an average imaging session of 45 minutes and 10 minutes of combined L- and S-SAR imaging. Solar panels have 23 m<sup>2</sup> area in two wings that track the sun generating 4017 W at summer solstice. A 180 Ah lithium-ion battery is sized to meet L-SAR imaging during eclipse and L and S combined modes. The battery and solar strings are designed with one string failure margin. Power is conditioned by HFS3R shunt regulators and fed to the bus. Charge and discharge regulators control battery current in- an out-flows. Power electronics monitor and controls the power system. The system has heritage from GSAT 11, GSAT 19 spacecraft.

**On Board Computers (OBC)**—The OBC is the main controller performing autonomous operations including command and telemetry processing, ACS functions, heater and temperature control, spacecraft health monitoring and fault response. It controls and triggers all other subsystems including payload controllers. It uses a SPARC-v8 LEON-3FT processor UT699 Realized using ASICs and FPGAs with hot redundancy. It is also the bus-controller for the 1553.

**S-band Telecom System**—S-band receivers are hot redundant; transmitters are cold redundant. S-band uses two omni antennas and supports coherent and non-coherent modes. Coherent mode supports ranging. OBCs provides baseband processing and are cross-strapped S-band.

**BDH and ISRO Ka-band Telecom**—The BDH CCSDS formats the S-SAR data and stores in the SSR. During playback through ISRO's Ka chain, the BDH retrieves SSR data, performs Reed-Solomon and trellis-coded modulation encoding and sends data to the Ka transmitters. The BDH supports 4.3 Gbps bust data in four chains. It also supports S-SAR telemetry and deployment camera video data.

ISRO's Ka-band system uses three data transmitters for RCP and three for LCP. Each transmitter has a data rate of 480 Mbps and uses 8PSK modulation. RF outputs of the three transmitters are combined using a 3:1 waveguide multiplexer.

*Dual Gimbal Antenna (DGA)*—JPL and ISRO Ka chains radiate to ground stations by a common DGA that is an upgrade of units on earlier ISRO missions. NISAR’s DGA will also be flown on ISRO’s CartoSat missions. A 0.7 m axially-displaced ellipse antenna is mounted on the DGA mechanism and fed by a rotary joint and septum polarizer. DGA articulates  $\pm 90^\circ$  about roll and pitch axes.

*Key Trades, and Challenges*

Major challenges accommodated by the spacecraft design include: a) the 12-m reflector; b) radar power; c) radar data volume; d) bus and payload controller handshaking; e) payload and bus thermal interface; and f) GSLV mass and volume constraints.

The reflector blocked the observatory’s negative yaw side which drove design and mission operation changes. Narrow fields of view are available for star sensors placement and baffles were redesigned from  $40^\circ$  to  $30^\circ$  sun rejection. ACS accommodates 10 min sun entry into the field of view in one of the three sensors while the other two meet requirements (only one sensor is needed to maintain pointing).

The reflector causes multipath to the omni antennas (one LCP and one RCP). LCP from the ground is reflected into the other omni in RCP. Downlink signals are also effected forming nulls on ground. A switchable antenna on positive yaw side was added to mitigate these effects.

ISRO heritage uses  $4\pi$  sun sensors for safe mode. This could not be accommodated because of reflector blockage. Safe mode is implemented using narrow field of view sensors (micro digital sun sensors). The safe mode algorithm was charged to sun search by rotating observatory about pitch and roll axes.

A large center of gravity shift occurs when the reflector is deployed. Thruster locations were optimized to accommodate all stages of deployment.

Battery and solar panel sizing balance electrical energy throughout the mission life considering string failures and end of life characteristics. Solar panel size is optimized to address shadowing by the payload structure and eclipse season imaging strategy.

**9. SYSTEM INTEGRATION AND TEST APPROACH**

System Integration and Test (SIT) is conducted in four phases plus a parallel mechanical I&T phase to qualify the shared structure, antenna support, boom and reflector has shown in Figure 9-1.

The first phase, now underway at JPL and SAC, is SAR I&T (SIT 1) where each SAR is assembled and tested standalone. Because JPL is providing the shared instrument structure, the L-SAR is integrated into that structure directly. The S-SAR is integrated onto a

portion of the structure provided by JPL (the “clamshell”). Functional and performance tests are conducted as described earlier.

In SIT2, S-SAR on its clamshell is shipped from SAC to JPL where it is integrated into the radar payload. S-SAR clamshell is integrated with the instrument structure followed by the L- and S-feed arrays. After integration, the radars complete a baseline radiating test to establish an end-to-end performance baseline. A joint compatibility test is conducted to ensure there is no degradation to system performance or timing, and verify commanding and data acquisition.

Key challenges in SIT2 are operating the radar in transmit mode and scanning the feed arrays to measure gain and phase across the aperture while radiating into an RF absorber wall. A precision scanner and RF probes will inject and receive chirps from a target simulator. A fiber optic delay line will be used to test the radars end-to-end. These measurements are complicated by having 24 receive beams that must be captured separately to verify DBF coefficients in the signal processors. A precision load box directs signals from any two radar channels to test equipment to monitor transmit waveforms. An antenna range test will measure antenna feed patterns. The passive antenna feed patterns will be combined with single-axis antenna scans to ensure that transmitted signals have proper phasing between channels and that calibration loops maintain phasing over a data takes.

During SIT1/2, a parallel effort (also now underway at JPL) qualifies the instrument antenna elements—the flight antenna support structure, flight boom and flight reflector on a flight spare structure which includes structural/ thermal simulators for electronics and flight heaters. This phase includes boom and reflector deployment tests, sine vibration test for launch requirements, and thermal vacuum and thermal balance tests in JPL’s solar simulator facility (where first motion deployment tests of the boom and reflector are performed). After thermal vacuum tests, the boom and reflector are removed for deployment tests at NG Astro, restored, and returned to JPL for SIT3.

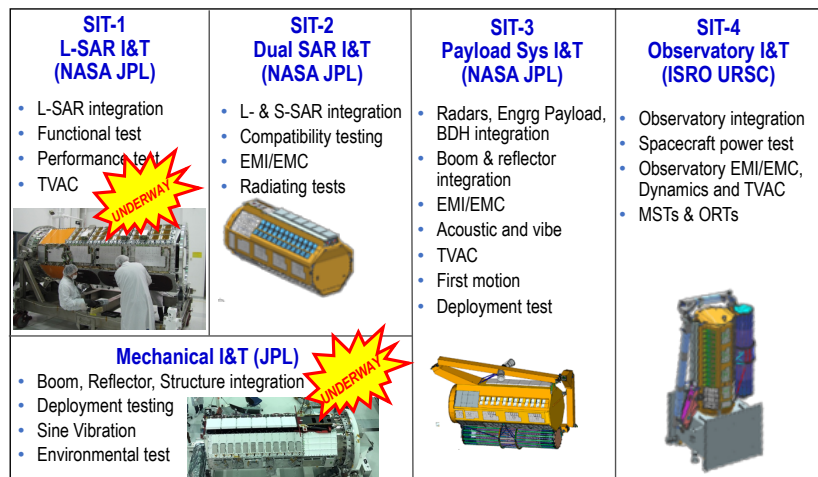


Figure 9-1. NISAR Integration and Test Flow.

In SIT3 at JPL, the boom and reflector are integrated with the instrument to complete the Radar Payload build-up. The Engineering Payload is integrated with the Radar Payload to form the Payload System. ISRO provides mass/thermal sims and the baseband data handler to be integrated. From this point, all testing is done in a flight-like manner where commands are generated using the Ground Data System (GDS) and sent through a spacecraft simulator and the GDS displays both S-band and Ka-band telemetry.

After functional testing, the Payload System undergoes dynamic tests and thermal balance testing in the launch configuration. After thermal-balance, a reflector first motion test is performed at ambient conditions. The reflector is returned to Astro for a final deployment test and final stow for flight. The boom is deployed on the flight Radar Payload a final time using the Engineering Payload and then prepared for shipment. The Payload System (sans boom and reflector) undergoes a second thermal balance test for on-orbit science configuration. Test heaters simulate radar transmit power heat load but TRMs are not radiating in the chamber. Finally, a Mission Scenario Test (MST) will exercise flight and ground systems together to verify day-in-the-life operations.

SIT4 at URSC integrates the payload system and spacecraft mainframe. The Engineering Payload is integrated onto the mainframe as discussed earlier. Initially, electrical integration is carried out on unmounted open spacecraft panels (open mode testing). Once completed, the spacecraft is assembled with all flight subsystems and a closed mode test is performed, followed by EMI/EMC and thermal-vacuum testing. An MST is repeated where flight and ground segments are exercised. Next the radar boom and antenna is installed. Dynamic testing and launch release checkout are performed following a nearly identical test campaign that was used during the radar mechanical I&T and SIT3 test programs. Following the dynamics test, a reflector first motion test is performed and then the reflector and boom are stowed for launch. There is a final payload radiating test in the stowed configuration where there is blockage over the feed tiles (only one TRM transmitting at a time with RF absorber placed over the radiating elements to protect the hardware). An End-to-End Information System Test will verify flight and ground data paths. The Observatory is then shipped to the Satish Dhawan Space Center launch site.

## 10. LAUNCH VEHICLE

NISAR will be launched from the Satish Dhawan Space Centre, Sriharikota (SHAR) by ISRO's GSLV Mk-II (Figure 10-1) with a 4-meter fairing. The GSLV uses three stages and four liquid strap-on's and is ISRO's largest launch vehicle; it has been in development and use since 2001 with many successful launches [13]. The maximum lift-off capability



Figure 10-1. GSLV-Mk-II.

## GSLV: (S139+4L40H) + L40HT + CUS15 + OPLF

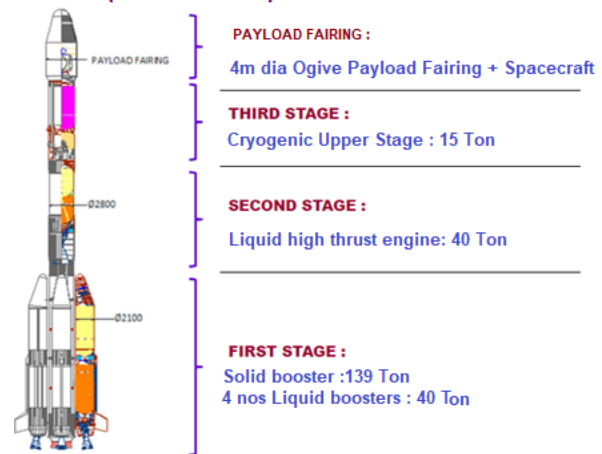


Figure 10-2. Configuration of GSLV Mark-II for NISAR.

Table 10-1. Mission parameters for launch vehicle

Spacecraft lift off mass	2612 kg
Orbit altitude	736 × 736 km
Orbit inclination	98.404 deg
Launch Azimuth	140 deg
Launch Station	SDSC SHAR

is 2612 kg based on successful historical flight data; this value is used as the growth limit for the observatory (including propellant). Mission analysis is carried out using this value.

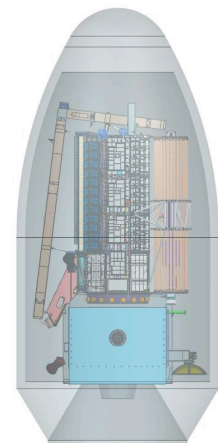


Figure 10-3. NISAR in GSLV 4-m Fairing.

The GSLV Mark-II configuration for NISAR is in Figure 10-2. This configuration will have at least two flights before NISAR in 2022. However, NISAR will be the first GSLV launch into low Earth orbit. The accommodation of NISAR inside the payload fairing can be seen in Figure 10-3.

Mission parameters for the vehicle are in Table 10-1. To avoid a conjunction probability with the final stage during the mission life, NISAR's injection orbit is 736 km; 11 km less than its science orbit (747 km). The spacecraft is boosted into the science orbit using spacecraft's propulsion system and fuel, nominally 12 days after the launch, after reflector deployment. The launch vehicle is continuously tracked from lift-off up to spacecraft separation using ISRO's tracking stations at SHAR, Trivandrum, and Mauritius.

## 11. MISSION OPERATIONS

ISRO and JPL share operational responsibility (Table 11-1, Figure 1-2). Satellite operations are conducted by ISRO's Telemetry Tracking and Command Network (ISTRAC) in Bengaluru. Science planning operations are conducted by JPL where a coordinated L-/S-SAR science observation plan developed with the science team based on the reference mission design. JPL and ISRO develop command sequences

**Table 11-1. ISRO and NASA/JPL Operational Responsibilities.**

Category	NASA/JPL	ISRO
Health and Performance Analysis	Perform for JPL-provided components and lead anomaly response for JPL components	Perform for ISRO-provided components and lead anomaly response for ISRO components
Orbit Determination (OD)	Provide GPS-derived OD products to support operations and science processing	Provide S-Band-derived OD products when GPS products are not available
Maneuver Planning	Plan and design science orbit maintenance and risk mitigation (per conjunction analysis) maneuvers; relay to ISRO for execution	Plan, design and execute maneuvers to achieve science orbit; execute science orbit maintenance and risk maneuvers
Science Planning	Maintain reference mission with science team inputs Generate coordinated L- and S-SAR science plan Generate L-SAR commands Generate revised plans for urgent response requests	Support coordinated science plan generation. Generate S-SAR commands from coordinated plan Deliver S-band SAR command products in response to request for urgent observations
Data Storage and Playback	Manage SSR storage and playback. Sequence commands for JPL-provided components	Sequence commands for ISRO-provided components
Ka-band Downlink	Downlink via NASA high-rate network L-SAR and select S-SAR data, and engineering payload data Perform NASA high-rate network scheduling	Downlink via ISRO high-rate network S-SAR and select L-SAR data Perform ISRO high-rate network scheduling
S-band Uplink and Downlink	Provide command products for JPL components Retrieve observatory S-band engineering telemetry from ISRO	Provide telemetry, tracking and command services via ISRO S-band ground network; receive and uplink JPL and ISRO commands; provide engineering telemetry to JPL
Data Transport	WAN from NASA ground stations to JPL processing sites for science data; and between ISTRAC and JPL for operations products (plan files, commands, telemetry)	WAN from ISRO ground stations to NRSC processing sites for science data; and to retrieve L- and S-SAR data from ASF or JPL science processor short term storage
Science Data Processing	Process L-SAR to L1 and L2; S-SAR to L0b Provide L-SAR L0a and L0b products to ISRO Prioritized processing of urgent response data to L0b	Process S-SAR to higher level products Process selected L-SAR to higher level products Provide S-SAR L0a and L0b to JPL
Data Archive	Deliver L- and S-SAR science products to ASF	Deliver L- and S-SAR science products NRSC

for their respective hardware. ISRO generates execution command files to be radiated to the observatory. L-SAR data is downlinked via Ka-band to NEN stations in Svalbard, Alaska and Wallops. S-SAR data and some L-SAR mission data is downlinked via ISRO Ka-band downlink to ISRO’s Integrated Multi-Mission Ground Segment for Earth Observation Satellites (IMGEOS) [14] complex at the National Remote Sensing Centre (NRSC) in Shadnagar and via ISRO’s Antarctic Bharati Station at Larsemann Hills. L-SAR data processing is conducted by JPL; data products are archived and distributed from NASA’s Alaska SAR Facility (ASF). S-SAR data processing is conducted by SAC; data products are archived and distributed by NRSC.

*Commissioning*

After launch, the mission enters a 90-day commissioning phase where checkout of spacecraft subsystems, deployment of the boom and reflector, maneuvers to reach science orbit, and checkout of the full observatory is completed [15]. The commissioning timeline is in Figure 11-1. Commissioning is divided into five sub-phases consisting of Initial Checkout, Deployments, Engineering Checkouts, Instrument Checkouts, and Observatory Checkout. Philosophically, the sub-phases are designed as a step-by-step buildup in capability to full Observatory operations.

*Science Operations*

Science operations is near-continuous instrument data collection and return that repeats over a 12-day cycle. The

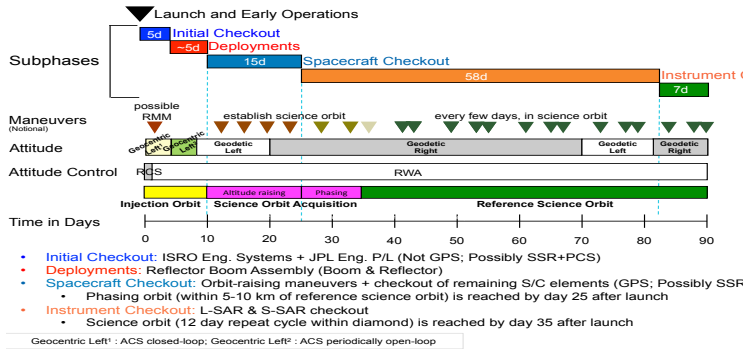


**Figure 11-1. Commissioning Timeline.**

observatory is gravity-gradient-minimized (~16 degrees rolled off nadir) except for brief periods when propulsive trim maneuvers are required to maintain orbit. During the first five months of science phase, calibration and validation (Cal/Val) of the data products is conducted. The observation plan for L- and S-SAR, along with plans for engineering activities (e.g., maneuvers, parameter updates, etc.), is generated pre-launch as the “reference mission;” the science observations within that reference mission are called the “reference observation plan.” The schedule of science observations is driven by L- and S-band target maps provided by the science team, radar mode tables, and spacecraft constraints and capabilities. Occasional updates to the reference mission are managed between the Joint Science Team and the Project.

*Science Data Processing*

Science data processing poses a particular challenge because of the unprecedented volume of science data that is returned

each day. JPL and ISRO are responsible for processing and archiving L- and S-SAR data and products, respectively. The Project is required to deliver L0B products to ASF within 24 hours of receiving data at JPL. Data products and associated volumes were described in the Mission Science section.

The mission will process products to L2, which is suitable for ingesting into downstream science and application processors to produce higher level products. To accommodate the data volumes required, the Project is utilizing Amazon Web Services (AWS<sup>®</sup>) Cloud Computing Services to provide for flexible assignment of General Processor Units (GPUs) instances and large data storage at an affordable cost.

## 12. CONCLUSION

The NISAR mission has been carefully designed to address a number of unique challenges posed by the mission objectives. The design ensures that NISAR will provide high-quality science data.

## ACKNOWLEDGEMENTS

The work described in this paper was carried out at the Jet Propulsion Laboratory, California Institute of Technology, under a contract with the National Aeronautics and Space Administration and at the Indian Space Research Organisation Space Applications Centre and the U R Rao Satellite Centre.

## REFERENCES

[1] Earth Science and Applications from Space: National Imperatives for the Next Decade and Beyond, Committee on Earth Science and Applications from Space, Ed., National Research Council, Washington, DC: The National Academies Press, 2007. ISBN 978-0-309-10387-9

[2] Thriving on Our Changing Planet: A Decadal Strategy for Earth Observation from Space, National Academies of Sciences, Engineering, and Medicine, Washington, DC: National Academies Press, 2018. <https://doi.org/10.17226/24938>.

[3] NASA JPL NISAR website: <http://nisar.jpl.nasa.gov>

[4] Implementing Arrangement between the National Aeronautics and Space Administration (NASA) of the United States of America and the Indian Space Research Organisation (ISRO) of the Republic of India for the Cooperation on the NASA-ISRO Synthetic Aperture Radar (NISAR) Mission for Scientific Studies of Earth, signed September 30, 2014.

[5] NASA. Responding to the Challenge of Climate and Environmental Change: NASA's Plan for a Climate-Centric Architecture for Earth Observations and Applications from Space, 2010.

[6] NASA-ISRO SAR (NISAR) Mission Science Users Handbook, Version 1, August 2019. <https://nisar.jpl.nasa.gov/files/nisar/NISAR%20FINAL%209-6-19.pdf>

[7] NASA JPL UAVSAR website: <http://uavsar.jpl.nasa.gov>

[8] G. Sadowy, H. Ghaemi, S. Hensley, "First Results from an Airborne Ka-band SAR using SweepSAR and Digital Beamforming," 2012 9th European Conference on Synthetic Aperture Radar (EUSAR), pp. 3–6, February 2012. ISBN: 978-3-8007-3404-7

[9] S. Huber, M. Younis, A. Patyuchenko, G. Krieger, A. Moreira, "Spaceborne Reflector SAR Systems with Digital Beamforming," IEEE Transactions on Aerospace and Electronic Systems, pp. 3473–3492, October 2012.

[10] S. Huber, M. Younis, A. Patyuchenko, G. Krieger, "Digital Beam forming techniques for spaceborne reflector SAR systems," EUSAR, pp. 962–965, 2010.

[11] S. Huber, M. Younis, A. Patyuchenko, G. Krieger, "A novel digital beam forming concept for spaceborne reflector SAR System," Proceedings of 6th European Radar Conference, pp. 238–241, October 2009.

[12] A. Reichert, T. Meehan, T. Munson, "Toward Decimeter-Level Real-Time Orbit Determination: A demonstration using SAC-C and CHAMP Spacecraft," ION, 2002.

[13] ISRO GSLV public website: <https://www.isro.gov.in/launchers/gslv>

[14] D. S. Jain, K. V. Ratnakumar, and M. Satyanarayana, Development of Integrated Multi-mission Ground segment for Earth Observation Satellites (IMGEOS), vol. 23, pp. 61–69. 2013.

[15] P. Sharma, "Updates in Commissioning Timeline for NASA-ISRO Synthetic Aperture Radar (NISAR)," 2019 IEEE Aerospace Conference, Big Sky, MT, USA, 2019.

## BIOGRAPHIES



**Kent Kellogg** has a B.S. (Electr Engrg, Cal Poly, San Luis Obispo '83). He is JPL's NISAR Project Manager. He has managed large project, program and functional organizations at JPL including SMAP; JPL's Telecom, Radar and Tracking Division; and SeaWinds and QuikSCAT.



**Paul Rosen** (S/'78, M/'03, SM/'05, F/'10) has PhD (Elect Engrg, Stanford). He is JPL's NISAR Project Scientist. He coordinates NASA's Surface Deformation and Change Decadal Survey Architecture Study. He led many JPL radar instruments

and applications developments. He is a Caltech visiting faculty member and has over 40 journal and book chapter publications and a 100 conference papers. He is IEEE Geoscience and Remote Sensing Society Director for Global Activities.



**Dr Raj Kumar** has a M.S and Ph.D. (Physics, Lucknow Univ). He has 35 years' experience leading activities to understand Earth System, processes and interactions using observation data, and its applications towards societal benefits as well as studies in Planetary sciences. He has conducted research on effective utilization of space technology, especially microwave remote sensing, for the ocean studies and atmosphere and climate for societal benefits. He has more than 90 publications and is leading many young researchers towards their Ph.D.



**Phil Barela** has a M.S. (Engineering, Loyola Marymount). He is NISAR's Deputy Project Manager with 27 years' experience. He managed Space Technology 7 with LISA Pathfinder; Mid-Infrared Instrument (MIRI) planned for JWST; ExoMars Trace Gas Orbiter; and WFIRST. He was project engineer at Loral and hybrid microelectronics engineer at Gould.



**Wendy Edelstein** has a B.S. (Electrical Engineering, Univ of California, San Diego '88). She is the NISAR Instrument Manager. She was SMAP Instrument Manager; Radar Science & Engineering Section Deputy Manager; Advanced Radar Technology Group Supervisor; and a Cognizant Engineer for SIR-C.



**Pamela Hoffman** has a B.S. (Mech Engineering, Berkeley '87) and M.S. (Caltech '89). She is NISAR's Deputy Instrument Manager. She was Mech Systems Asst Division Manager, SMAP Instrument Mechanical System Manager; MSL Cruise Entry Descent and Landing Mechanical System Manager, Cruise Stage Cog-E on MER, and thermal and launch vehicle integration on Cassini.



**Shaun Standley** has a B.S. (Aeronautics and Astronautics, Southampton Univ, UK) and a MBA (Pepperdine). He is a INCOSE Expert Systems Engineering Professional. He is NISAR's Project System Engineer. He was system engineer on Kepler, Cassini, Huygens Titan probe, Ulysses, and for technology



development. He supervised the System V&V Group. He also worked on UK's Skynet 4B, Eutelsat 1-F4 and Eutelsat 1-F5.

**Ana Maria Guerrero** has a B.S. (Computer Science, Cal State LA). She joined JPL in '86 and is NISAR's Mission System Manager. She was Deep Space Network Tracking, Telemetry, Command Operations Manager, Multi-Mission Ground Data Systems Group Supervisor, and Uplink Task Development Manager.



**Charles Baker** has a M.S. (Aerospace and Mechanical Engineering, Univ of Colorado '03). He joined JPL in '06 and is now NISAR's Mission Systems Engr. He was MSL's Mission Planning Lead, SMAP Fight Ops Engineer, Mars 2002 Mission Planner and Instrument Special Applications Group supervisor.



**V Raju Sagi** has a B.E. (Electronics & Comm, JNT Univ, Kakinada '83), and a M.S in Comm Systems (PSG College of Tech, Coimbatore '85). He joined ISRO's Satellite Centre in '85 working on Measurements and Satellite RF & Comm Systems Test Automation. He is Project Director for Resourcesat-2A and NISAR.



**Rakesh Bhan** has a B.E. (Electronics and Communication, Amravati Univ '00) and is the Associate Project Director for NISAR's S-SAR. He is Lead for L&S Airborne SAR and Head of SAC's Microwave Sensors Systems Division. He was RISAT-1 SAR lead and is an Expert member of L&S Band Dual Frequency SAR for Chandryaan-2 and Ka-Band Altimeter teams. He's responsible for design and analysis, specifications, integration, V&V of SARs in L, S, C, and X bands. He holds 5 publications, 3 patents, 1 copyright.



**Yuhsyen Shen** has a Ph.D. (electrical engineering from U Penn '87). He has served leadership roles in radar-projects, including Air SAR, SIR-C/X-SAR, SRTM/X-SAR, CloudSat, AQ and RapidScat. He was NASA's Deep Space Network systems manager and Communications, Tracking and Radar Division deputy manager. He is now the NISAR chief engineer.



**Peter Xaypraseuth** has a B.S. (Aerospace Engrg Cal Poly, Pomona, '00). He is NISAR's Flight System Systems Engineer overseeing the Engineering Payload design and ISRO spacecraft interfaces. He has had system and mission roles on Mars Reconnaissance Orbiter, Dawn, and GRAIL.



**Charles Dunn** has a B.S. (physics, Univ. of Wash, '85) and Ph.D. (physics, Cornell '90). He is NISAR's Flight System Manager. He was JPL's Flight Communications System Section Manager, Tracking and Applications Section Deputy Manager, Project Engineer for ST7 on LISA Pathfinder, Payload Manager of GRAIL, and GRACE Instrument Manager.



**Scott Shaffer** has a B.S. (electrical engineering Univ of Calif, Davis '84), and a M.S (UCLA '86). He's worked on airborne and spaceborne radars including SIR-C, Magellan, SRTM, UAVSAR, and Cassini. He was lead engineer for Pathfinder, MER, Phoenix landing radars. He is the NISAR L-SAR System Engineer.



**Nandini Harinath** is Mission Systems lead for NISAR and RISAT-2A. She is Deputy Operations Director for Mars Orbiter Mission (MOM) and Mission Director for RISAT-2B and ResourceSat-2A. She has a number of publications and awards including "India Today Woman in Science Award 2015," Astronomical Society of India Team Award for Mars Orbiter Mission 2014, ISRO's Team Excellence Award for RISAT-1.\



**C. V. H. S. Sarma** has a B.S. (Electronics & Communication (Inst of Electronics & Communication Engineers, New Delhi, '95) and M.S. in Software Systems (Birla Inst of Tech, Pilani, '00). He is URSC's Deputy Project Director-Electrical Systems for NISAR & RISAT-2A. Previously he was Project Manager for several spacecraft and for GPS-Aided GEO Augmented Navigation (GAGAN). His experience includes reliability, safety analysis, test & evaluation, product assurance, integration & test, and operations.